Electronic Supplementary Material (ESI) for Lab on a Chip.

Supporting Information

A Fast and Switchable Microfluidic Mixer Based on Ultrasound-Induced Vaporization of Perfluorocarbon

Marine Bezagu,[§,†] Stellios Arseniyadis,*[†] Janine Cossy,*[†] Olivier Couture,[‡] Mickael Tanter,[‡] Fabrice Monti,[§] and Patrick Tabeling*[§]

[§]Laboratoire de Microfluidique, MEMS et Nanostructures
ESPCI ParisTech, CNRS (UMR Gulliver 7083), Paris, France

[†]Laboratoire de Chimie Organique, Institute of Chemistry, Biology and Innovation (UMR 8231),
ESPCI ParisTech/CNRS/PSL* Research University

[‡]Institut Langevin, ESPCI ParisTech, CNRS (UMR 7587), INSERM (U979), Paris, France

Materials: Nile Red and mineral oils were purchased from Sigma Aldrich. Fluorescent beads (10 µm in diameter) were purchased as a suspension in water from Invitrogen. Perfluorohexane came from 3M (FC-72), and perfluoropentane from FluroMed.

Microfluidic device fabrication: The devices are made in PDMS (polydimethylsiloxane), using the standard soft lithography technique. In brief, we create SU8 (SU8 2015, Microchem) masters on a silicon wafer, then proceed to PDMS (RTV615, Momentive Performance Materials) molding and thermal curing at 80 °C overnight. We treat the PDMS surfaces and the glass slide that closes the channel with oxygen-plasma before sealing in order to obtain excellent adhesion and ensure a hydrophilic behavior. When using the systems with hydrophobic liquids such as mineral oil, the hydrophobicity of the PDMS surface was obtained by leaving the systems in a 90 °C oven overnight. The microfluidic system is then physically connected with small tubing (Tube PEEK 1541, Idex Health and Science) to a syringe pump (neMESYS low pressure syringe pump, Cetoni). The flows are visualized using an inverse microscope (Leica). The main channels are 150 µm in width and 14 µm in height.

Figure S1. System geometry: Full system is drawn to scale and the geometric characteristics of noteworthy regions are given.

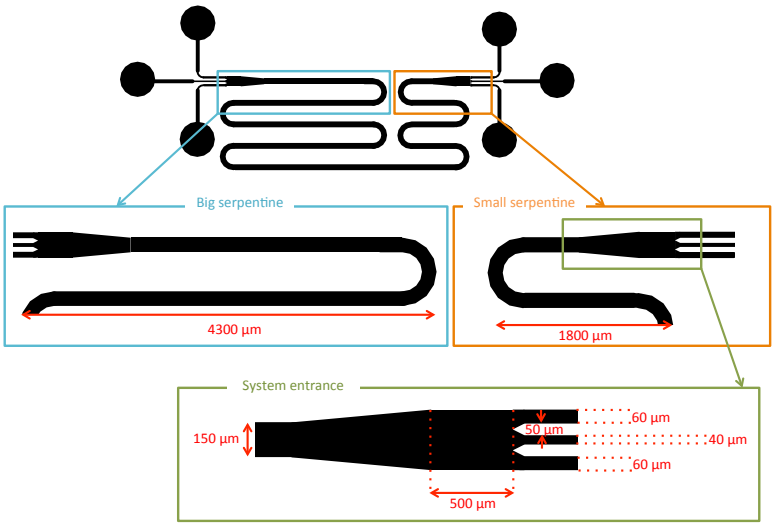

Experimental set-up: For all experiments, fluids were injected in a microfluidic system made of polydime-thylsiloxane (PDMS) on glass with a uniform channel-height of 14 µm. A 2.25 MHz mono-element transducer (focus = 38 mm, f/d = 1) was focused within the channel emitting pulses of 1 to 40 cycles spaced out every 100 µs to 1 ms. The amplitude of the pulses can be modulated from 4.6 to 9.1 MPa peak-negative pressure, before being amplified by a radio-frequency amplifier. An EM-CCD camera (Andor, iXon) mounted on a fluorescent microscope (Leica, 4X with a Leica 11513880 filter) recorded the fluorescence evolution during and between mixing events.

Figure S2. Experimental set-up

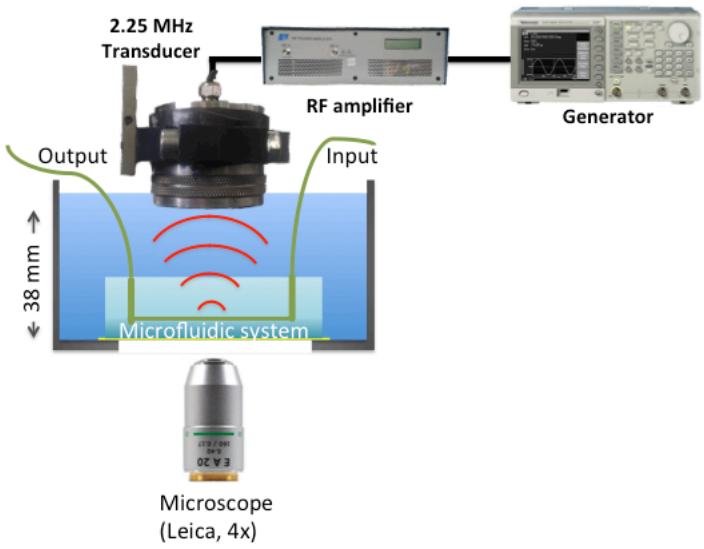

Three cases were studied:

Method A: three fluids are injected, respectively Nile Red in mineral oil (600 µM), 1:1 perfluoropentane/perfluorohexane mixture (PFC) and pure mineral oil.

Method B: three fluids are injected, respectively 10 µm beads in mineral oil, 1:1 perfluoropentane/perfluorohexane mixture (PFC) and pure mineral oil.

Method C: three fluids are injected, respectively fluorescein in water (800 µM), 1:1 perfluoropentane/perfluorohexane mixture (PFC) and pure water.

Figure S3: Cases Studied

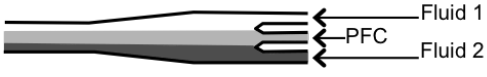

Method	Fluid 1	Fluid 2
Method A	600 µM Nile Red in mineral oil	Pure mineral oil
Method B	10 µm fluorescent beads in mineral oil	Pure mineral oil
Method C	800 µM fluorescein in water	Pure water

Nile Red concentration study: We observed the fluorescence of different solutions of Nile Red in mineral oil at different concentrations (Figure S4). As no auto-quenching phenomenon was observed, we chose to work at the maximum concentration to get the highest signal on the camera (400 µM).

Figure S4

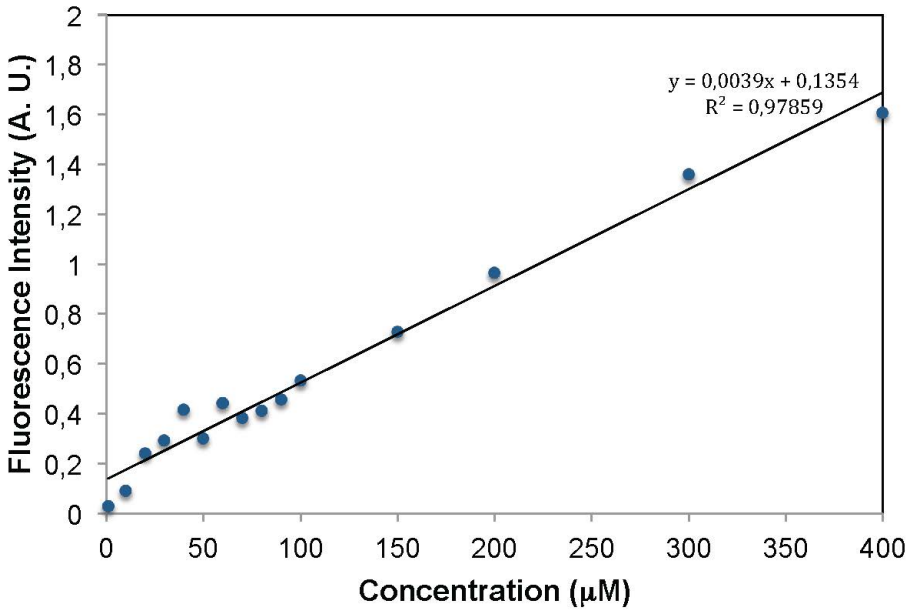

Fluorescein concentration study: We observed the fluorescence of different solutions of fluorescein in water at different concentrations (Figure S5). Considering the auto-quenching effect on the fluorescence intensity beyond 10 mM, we focused our attention on the 0-1 mM range of concentrations.

Figure S5

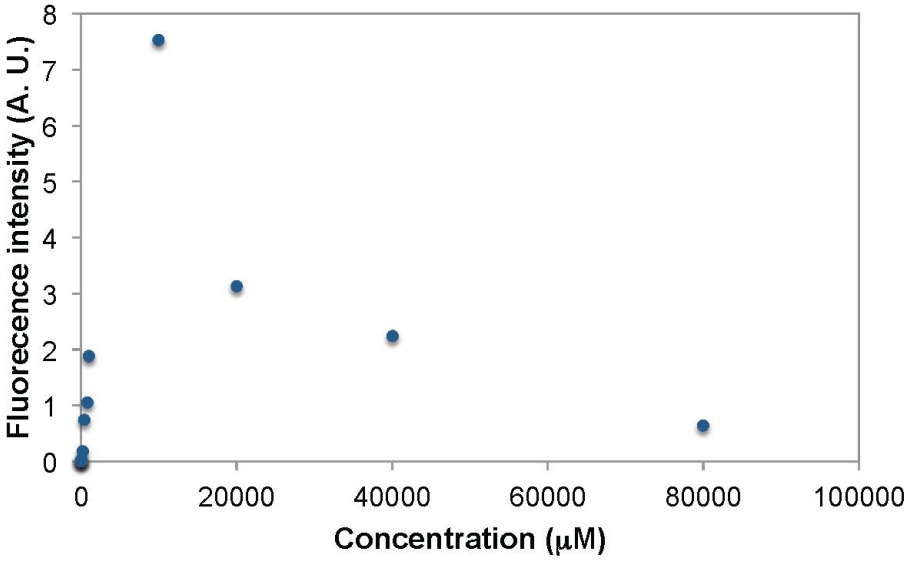

We chose to work at a concentration of 800 µM in fluorescein, which appeared to belong to the linear progression of intensity *vs* concentration (Figure S6).

Figure S6

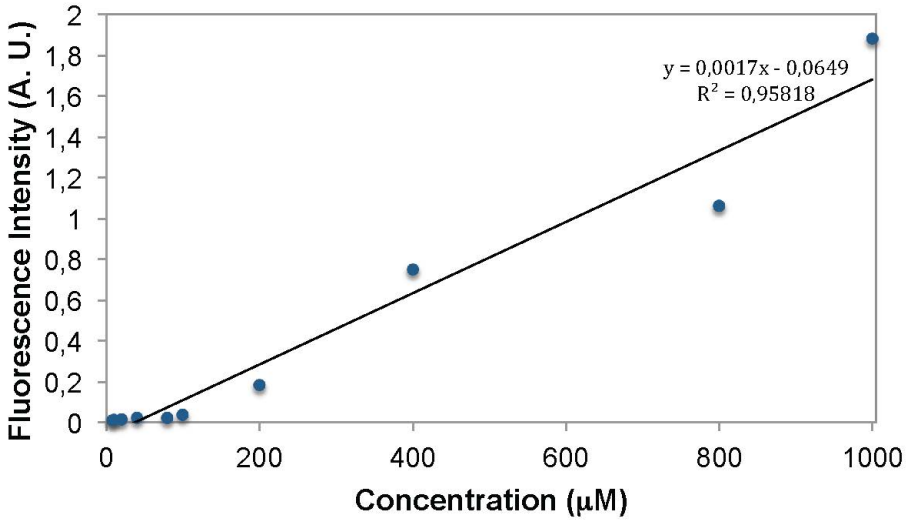

Fluorescent beads suspension preparation: beads of 10 µm in diameter were initially purchased as a suspension in water. They were concentrated by centrifugation, before 5 µL of these concentrated beads were transferred in 10 mL mineral oil. This mixture was sonicated for 60 min before each experiment and injected directly in the microfluidic channel.

Data treatment: Matlab software was used for all data treatment. In particular, we were able to define two zones (**blue** and **green** boxes) of 39 pixels each, in which we followed the evolution of the pixels' intensity over time (Figure S7).

Figure S7

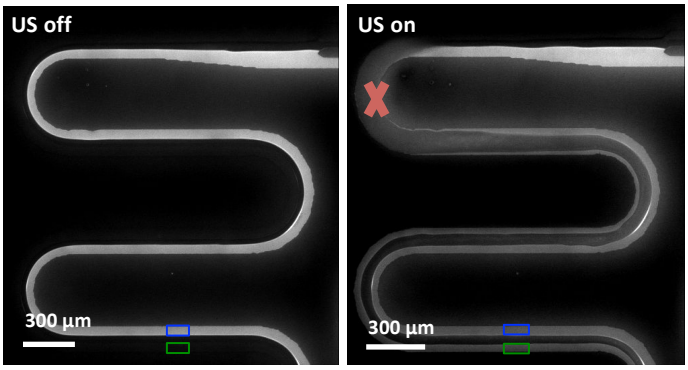

The average fluorescence of these regions was recorded over the sequence of images. In the absence of ultrasound pulses the two external phases remain well separated by the non-miscible central PFC layer and the average fluorescence of both regions remain unchanged independently of the case studied until ultrasound excitation (**Method A**, Figure S8 and Table S1 and **Method C**, Figure S9).

The evolution of the average intensity in both zones over time is represented on the graphs below on two examples:

Hydrophobic system (Re=0.023)	**Hydrophilic system (Re=1.7)**
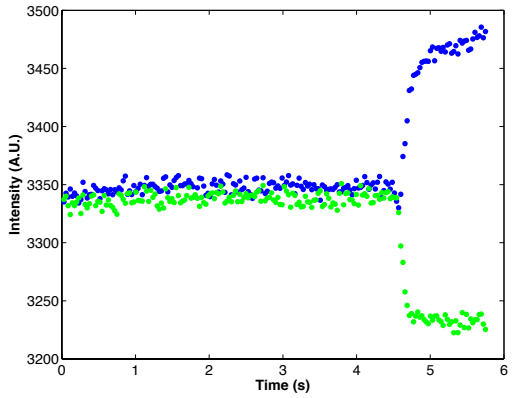	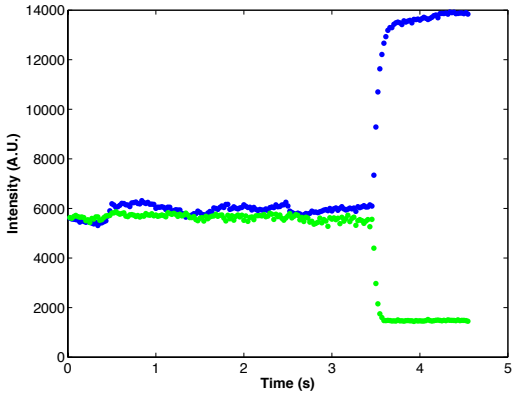

The mixing index was calculated according to the following equation, after normalization of the intensities:

$$MI = \sqrt{\frac{1}{N}\sum_{1}^{N}\left(\frac{I_i - \langle I \rangle}{\langle I \rangle}\right)^2}$$

Where N is the total number of pixels in the selected zones, I_i the intensity of pixel *i* and <I> the average intensity over the *N* pixels.

Mixing index evolutions of the two examples developed here are shown on Figure S8 and S9 (hydrophobic and hydrophilic cases respectively). Average values of mixing index for other hydrophobic systems are gathered in Table S1. We used standard deviation tool to express the mixing index fluctuations around the average value.

Figure S8: Representative fluorescence microscopy images corresponding to mixing following **Method A**. Ultrasound focus is represented by the red cross. Corresponding mixing index evolution (Q_{oil} = 2.5 µL/min, Q_{tot} = 25 µL/min, v_{oil} = 36.10^{-6} $m^2.s^{-1}$, Re = 0.023)

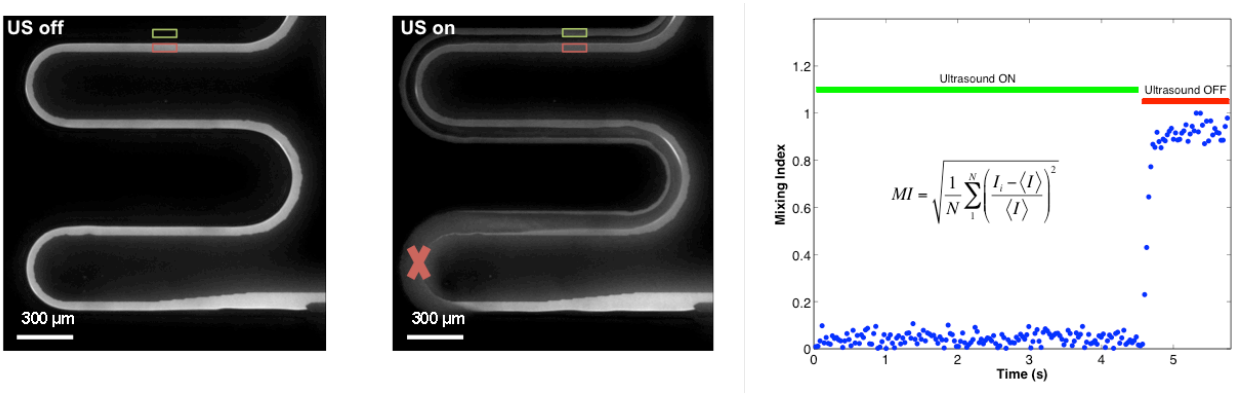

Figure S9: Representative fluorescence microscopy images corresponding to mixing following **Method C** (with or without ultrasound activation). Focal zone represented by the red cross. Corresponding mixing index evolution (Q_{water} = 5 µL/min, Q_{tot} = 18 µL/min, v_{water} = 1.10^{-6} $m^2.s^{-1}$, Re = 1.7).

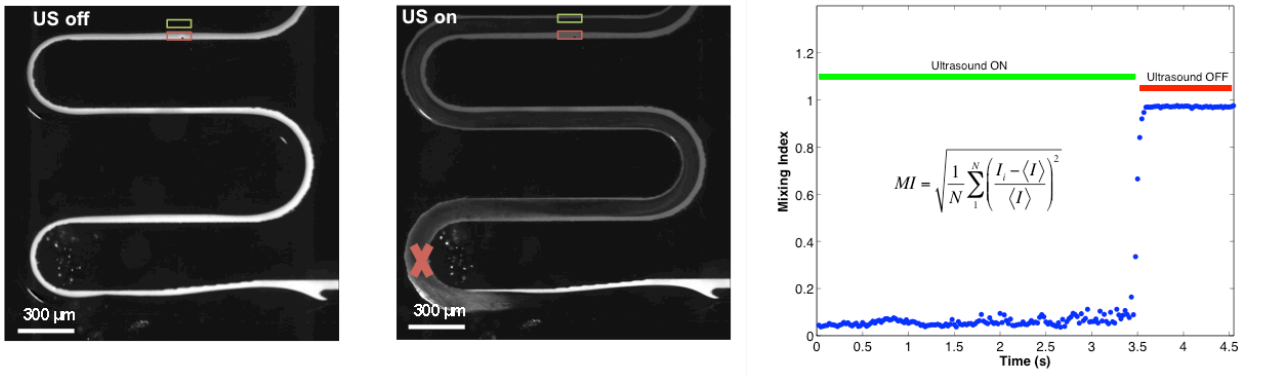

Table S1: Mixing following **Method A** and corresponding mixing index evolution for different oils and flow rates

Kinematic viscosity ($m^2.s^{-1}$)	**Oil flow rate (µL/min)**	**Reynolds number**	**MI**	**Graph**
$v_{oil} = 1x10^{-6}$	0.6	2.10^{-1}	0.04±0.03	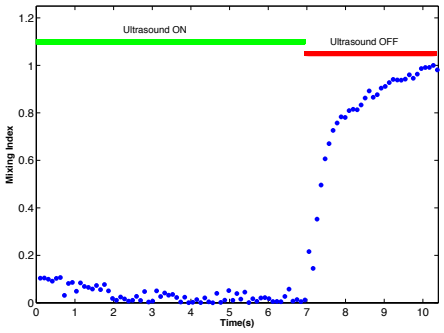
$v_{oil} = 1x10^{-6}$	0.8	$2.7.10^{-1}$	0.03±0.01	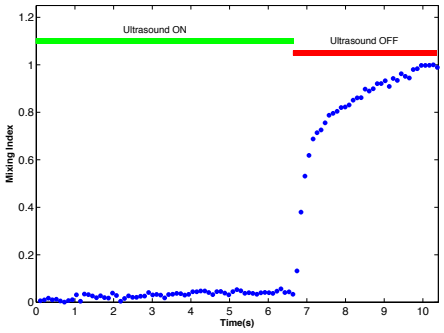
$v_{oil} = 1x10^{-6}$	2	$6.7.10^{-1}$	0.05±0.01	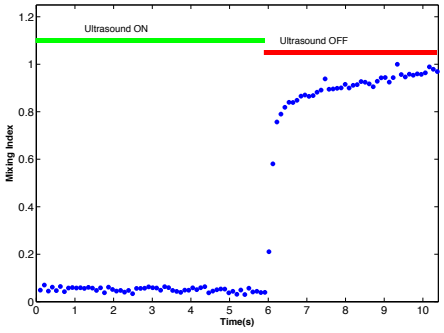
$v_{oil} = 16x10^{-6}$	0.1	$2.1.10^{-3}$	0.04±0.01	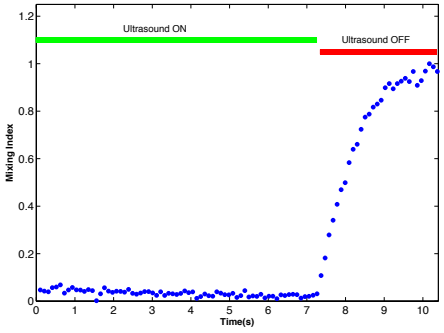

v_{oil} = 16x10^{-6}	1	2.1.10^{-2}	0.06±0.01	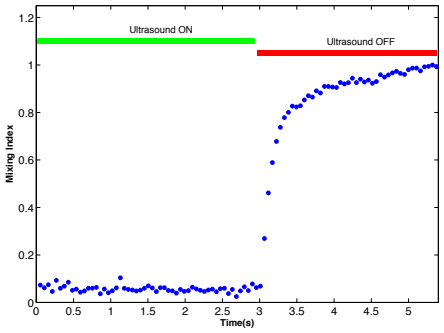
v_{oil} = 67x10^{-6}	0.1	5.0.10^{-4}	0.04±0.03	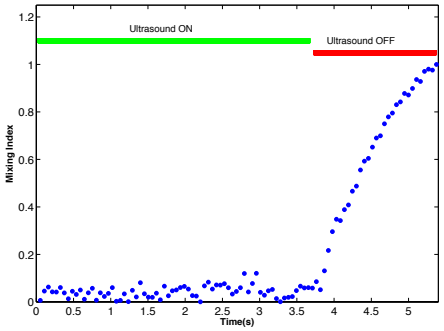
v_{oil} = 67x10^{-6}	0.03	1.5.10^{-4}	0.07±0.02	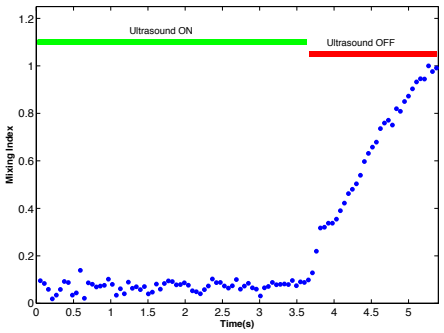

The transition between a mixing and a non-mixing situation remained unaffected upon increasing the total flow rate from 9,6 μL/min to 48 μL/min (corresponding to Reynolds numbers ranging from 0.0074 to 0.037), the splitting of the beads on both sides of the channel occurring in a similar fashion (Figure S10).

Figure S10. Mixing of two oil phases, according to Method B (beads in oil, v_{oil} = 36.10^{-6} m^2.s^{-1}) at different flow rate.

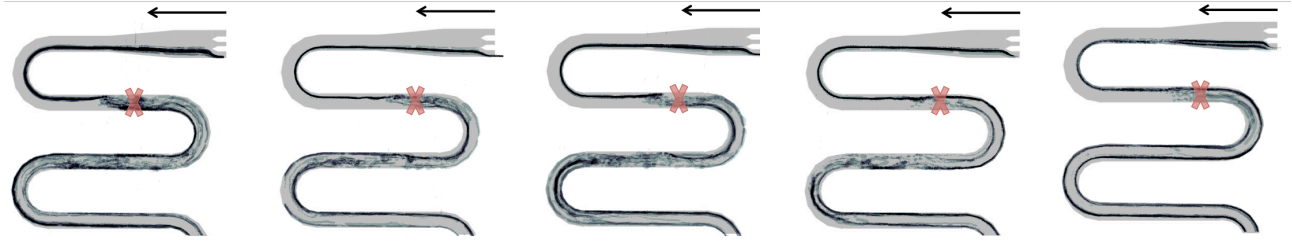

Q_{tot}= 9,6 µL/min **Q_{tot}= 12,4 µL/min** **Q_{tot}= 18 µL/min** **Q_{tot}= 24 µL/min** **Q_{tot}= 48 µL/min**

Study of the mixing kinetics. Matlab software was used for all data treatment. For each flow rate value, we defined a working zone (in **red**, see Figure below) corresponding to half of the channel's width. In the absence of ultrasound, all the fluorescent beads remain on the other side of the PFC layer outside the red box. In the presence of ultrasound, this box is progressively filled with fluorescent signal due to the deviation of the beads' trajectories under the focus of the ultrasound.

Figure S11

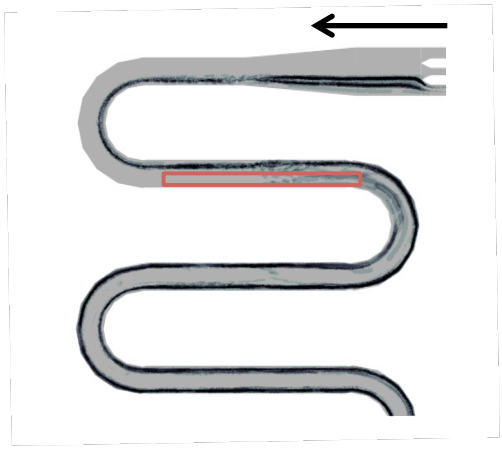

The intensity of each pixel of the red zone is represented in the Figure below. This half of the channel is initially empty from fluorescent beads (intensity equal to zero). It then starts to display positive fluorescence intensity as the beads start to cross the channel.

Figure S12

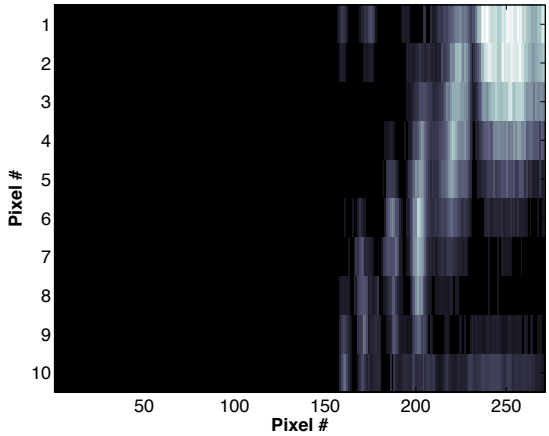

The intensity was summed along the width of the defined zone:

Figure S13

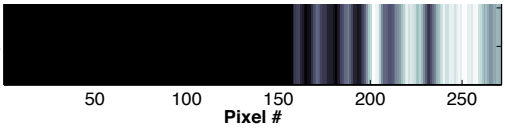

Finally, this intensity signal was fitted using a sigmoid function. Positions corresponding respectively to 10% and 90% of the sigmoid's maximum were used to evaluate for each flow rate the distance necessary to affect laminarity of the flow.

Figure S14

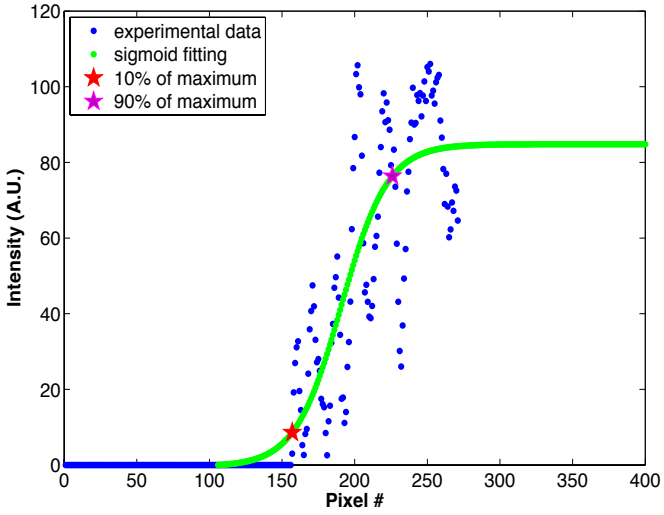

These distances were converted into corresponding times:

Flow rate	x10% (#pixels)	x90% (#pixels)	Time (ms)	Average time (ms)
9.6 µL/min	166	173	0.4	
12.4 µL/min	199	236	1.8	
18 µL/min	146	181	1.2	1. 2 ± 0.5
36 µL/min	148	249	1.7	
48 µL/min	157	226	0.9	

The average time necessary to affect laminarity was found to be equal to 1.2 ± 0.5 ms.